

# International Conference on Space Optics—ICSO 2022

Dubrovnik, Croatia

3–7 October 2022

*Edited by Kyriaki Minoglou, Nikos Karafolas, and Bruno Cugny,*



## *Comparative study with high-quality, functionally coated Alexandrite crystals for spaceborne LIDAR applications*



## Comparative study with high-quality, functionally coated Alexandrite crystals for spaceborne LIDAR applications

S. Unland<sup>\*a</sup>, R. Kalms<sup>a</sup>, P. Weßels<sup>a</sup>, T. Böntgen<sup>a</sup>, H. Mädebach<sup>a</sup>, M. Hunnekuhl<sup>a</sup>, D. Kracht<sup>a</sup>,  
M. Lorrain<sup>b</sup>, P.G. Lorrain<sup>b</sup>, M. Hmidat<sup>b</sup>, J. Butkus<sup>c</sup>, L. Lukoševičius<sup>c</sup>, J. Neumann<sup>a</sup>

<sup>a</sup>Laser Zentrum Hannover e.V., Hollerithallee 8, 30419 Hannover, Germany; <sup>b</sup>Optomaterials S.r.l.,  
Via Antioco Loru 15, 09125 Cagliari, Italy; <sup>c</sup>Altechna, Mokslininku g. 6A, 08412 Vilnius, Lithuania  
<sup>\*</sup>s.unland@lzh.de

### ABSTRACT

A lot of investigations are ongoing for the development of laser systems with Alexandrite as active laser medium. These laser systems fulfill the general laser requirements for spaceborne Earth observation missions such as altimetry. However, to date, the laser systems and especially the coated Alexandrite crystals do not exceed Technology Readiness Level (TRL) 4. Therefore, the Horizon 2020 project GALACTIC was initiated to develop reproducible, fully European supplier-based functionally coated Alexandrite crystals, which show at least the same optical quality and laser performance in comparison to the components from the leading suppliers on the global market (mainly US and Chinese companies) and further fulfill the qualification to be generally used in space (i.e. verification of TRL 6). We present the high optical quality and good laser performance results of our developed Alexandrite crystals tested in a cavity-dumped Q-switched laser system. Furthermore, we show on the one hand the reproducibility and on the other hand the competitiveness of our crystals by a comparison study with our GALACTIC samples and crystals from two non-European suppliers.

**Keywords:** Alexandrite, TRL 6, Earth observation, LIDAR, Diode-pumped laser, Solid-state laser, Space qualification

### 1. INTRODUCTION

Space-qualified Alexandrite laser crystals with their inherent optical and physical properties have shown to be promising candidates to be implemented for spaceborne Earth observation missions, e.g. due to a wide spectral emission range, high optical efficiency and beneficial properties such as high mechanical hardness and high thermal conductivity [1,2]. Therefore, it is not surprising that Alexandrite is intensively researched as alternative active laser medium for the use in remote sensing applications. Exemplary studies have been dealing with the development of single frequency Alexandrite lasers for potassium LIDARs [3,4] or frequency-doubled Alexandrite-based iron LIDARs to measure wind and temperature in the Mesosphere [5]. Furthermore, the Alexandrite laser properties allow for the generation of short pulses in the ns range with high repetition rates (kHz), which is also interesting for vegetation monitoring or altimetry. In a first approach by Thomas et al. [6], a cavity-dumped Q-switched Alexandrite laser was developed. Despite the wide range of investigations, the laser systems and especially the coated Alexandrite crystals however do not exceed TRL 4 [7].

Therefore, the H2020 project GALACTIC [8,9] has been initiated to establish a fully European supply chain for high-quality, functionally coated Alexandrite laser crystals, which will be qualified for TRL 6. In the first two years of the project, different technology areas were addressed to reach the GALACTIC goals. The crystal growth process as well as the cutting and polishing techniques were refined, and high-quality, low loss, high damage threshold coatings were developed. Details of the goals and planned tests in the course of the GALACTIC project can be read up in [10]. The coated Alexandrite crystals were tested in an enhanced cavity-dumped Q-switched laser system, adopted from the first approach already mentioned above. Suitable laser output parameters were defined for the performance study and summarized in Table 1. The table also contains the optimum achieved output parameters within this system up to now. This conference paper concentrates on the laser results achieved with the Alexandrite crystals manufactured within the GALACTIC project to verify the reproducibility of the crystal quality and the functional coating. To classify the European GALACTIC crystals in the global market, a comparison study was carried out regarding the laser performance and the laser-induced damage threshold (LIDT). For this purpose, crystals from two established non-European manufacturers were evaluated. A last step towards space-qualified components will be an environmental test campaign to push the development of Alexandrite crystals and coatings within the EU from the current TRL 4 up to TRL 6.

Table 1: List of requirements and measured laser parameters as well as for the environmental test campaign in GALACTIC.

	Requirement	Measured parameters
Output wavelength	$760 \pm 10$ nm	$755 \pm 3$ nm
Output energy	$\geq 200$ $\mu$ J	$> 500$ $\mu$ J
Pulse duration	$< 10$ ns	2.8 ns
Repetition rate	$\geq 5$ kHz	1 – 20 kHz
Lifetime	-	$> 8$ h (150 Mega shots)
Operational temperature range	-30 °C – 130 °C	
Rad. hardness: gamma (TID)	Dose levels: 10 & 30 krad; dose rate: 4 krad/h	
Rad. hardness: proton (TNID)	$10^{11}$ protons/cm <sup>2</sup> (23 & 68 MeV equivalent protons); proton flux rate: $8 \cdot 10^7$ protons/(cm <sup>2</sup> s)	

## 2. TESTED SAMPLES AND LASER SETUP

In order to obtain a meaningful result on the reproducibility and to verify a similar laser performance, coating and quality of the GALACTIC laser crystals, ten samples were employed for these studies, thereof eight for the laser performance tests and two for LIDT measurements. To classify their current competitiveness within the global market, four laser crystals each from two non-European suppliers (USA & China) were used for the comparison study, which is presented in Section 4. Details of the crystal specifications, labeling and coating are listed in Table 2.

Table 2: List of tested Alexandrite crystals and their specifications, used for the reproducibility and comparison study.

Manufacturer/suppliers	Labeling	Doping concentration	Dimensions	Coating
EU/ GALACTIC	EU sample #1 – EU sample #10	0.20 at%	4 x 4 x 10 mm <sup>3</sup>	AR < 1 % @ 638 ± 20 nm, AR < 0.25 % @ 760 ± 20 nm, AOI = 0°
USA	US sample #1	0.13 at%		
	US sample #2 – US sample #4	0.22 at%		
China	Chinese sample #1	0.13 at%		
	Chinese sample #2 – Chinese sample #4	0.22 at%		

The measurements were performed in the L-shaped cavity-dumped Q-switched laser system shown in Figure 1. In this system, the Alexandrite crystal was embedded in a thermoelectric cooler controlled copper mount with a temperature set to 30 °C. The crystal was pumped by a fiber-coupled laser diode offering maximum 40 W cw output power at a center wavelength of 638 nm. Two aspherical lenses were used to focus the unpolarized pump laser output into the crystal. The beam at the focus position had a super-Gaussian shape with a diameter of 320  $\mu$ m and an M<sup>2</sup> of ~200 in the horizontal and vertical direction. A retro-reflecting pump-optic was used to optimize the amount of pump absorption (90 %). The complete pump optic, including the fiber output coupling, was mounted on a linear translation stage, which enabled a precise adjustment of the focus position along the optical axis inside the crystal without changing the focus size or caustic. The L-shaped cavity was implemented using an input coupler (IC), a bending mirror (BM) and a highly reflecting end mirror (HR). Moreover, an intra-cavity plano-convex lens with a focal length of 125 mm was used to ensure a good overlap of the pump volume and the laser mode in the laser crystal. The resulting cavity length was around 340 mm. Cavity-dumped Q-switching was achieved by an integrated BBO Pockels cell in combination with a quarter-wave plate (QWP)

and a thin-film polarizer (TFP). The laser pulse inside the cavity built up during the switching-on time of the Pockels cell and was coupled out at the TFP by rapidly switching off the high voltage. During the measurements, the delay between switching on and off as well as the axial pump focus position were optimized to reach the maximum output energy. This procedure was carried out for every set pump power since the delay corresponds to the build-up time of the intra-cavity flux to reach its maximum.

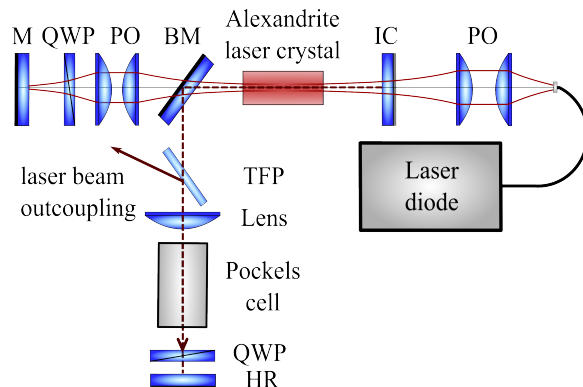


Figure 1: Schematic drawing of the cavity-dumped Q-switched Alexandrite laser with double pass diode pumping: M: mirror, QWP: quarter wave plate, PO: pump optics, BM: bending mirror, IC: input coupler, HR: highly reflecting mirror, TFP: thin-film polarizer.

### 3. LASER PERFORMANCE OF GALACTIC CRYSTALS

To demonstrate the specified lasing performance and verify the reproducible manufacturing process of the GALACTIC components, eight laser crystals (EU sample #1 – EU sample #8) were characterized at a fixed pulse repetition frequency (PRF) of 5 kHz regarding their output parameters. To avoid any damage of the crystals, the measurements were restricted only up to an absorbed pump power of 27 W, even though higher output energies are in general possible (see Table 1). The resulting laser pulse duration was 2.8 ns in all cases. The resulting laser output energy curves are depicted in Figure 2a. Except for the results achieved with EU sample #8, all curves show a nearly similar increase up to 400 – 450  $\mu\text{J}$ . The significantly different course of the energy increase measured with EU sample #8 could be caused by small defects detected on the front surface of the crystal, which led to higher absorption and scattering losses, in combination with a slightly worse alignment. Therefore, this result was not included in the calculation of the mean course shown as the black line in Figure 2a. The deviation between the measurements becomes larger for increasing pump power up to a maximum of  $\pm 7\%$ . These differences can be caused by stronger thermal effects inside the laser crystal due to higher absorbed pump powers, e.g. due to an increasing dioptric power of the thermal lens, which in return leads to the laser reacting more sensitively to the pump focus adjustment. Moreover, these thermal effects can be slightly different for each tested crystal.

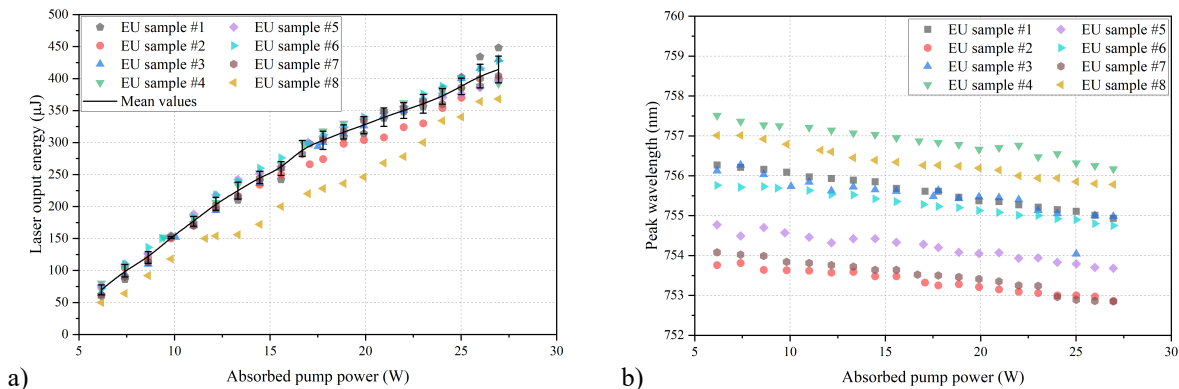


Figure 2: Comparison of the laser output performance measured with 8 GALACTIC samples. a) Laser output energy as a function of the absorbed pump power including the mean values determined from samples #1-7; b) Variation of the peak wavelength for all tested crystals with increasing absorbed pump power.

The peak wavelength of the Alexandrite laser as a function of the increasing absorbed pump power is illustrated in Figure 2b. The variation of the peak wavelengths for all considered crystals is similar in the scope of the measurement accuracy with a constant offset of maximum 5 nm. The difference between the resulting laser wavelengths can have different origins: One major cause could be a misalignment of the crystals' c-axis to the optical axis by the crystal cutting. The wavelength dependence on the angle of incidence either in the vertical or the horizontal direction towards the optical axis was investigated in detail in literature [11] and is induced by the birefringent properties of Alexandrite. Furthermore, the cavity was adjusted to the highest output energy after every change of the crystal, which could cause slight differences in the resulting laser beam path inside the cavity. Thereby, the angle of incidence related to the TFP could also be slightly different, which leads to a shift of the transmission minimum of the coating curve. A second potential reason can be traced back to the coating deposition on the crystals. A shift of the optimum wavelength in the order of 0.1 % can arise during the coating deposition just due to the position of the crystals inside the coating machine. With an optimum wavelength of 760 nm a shift of < 1 nm can be estimated in this case. In Figure 2b, it can also be observed, that the peak wavelengths measured with all considered crystals decrease for increasing absorbed pump power by about -0.06 nm/W due to the increase of the temperature inside the crystal, which was also observed in literature [11].

In general, it can be seen that small misalignments or variations in the crystal axis orientation can cause small differences in the spectral characteristics of the laser output beam, but do not affect the resulting laser output energy.

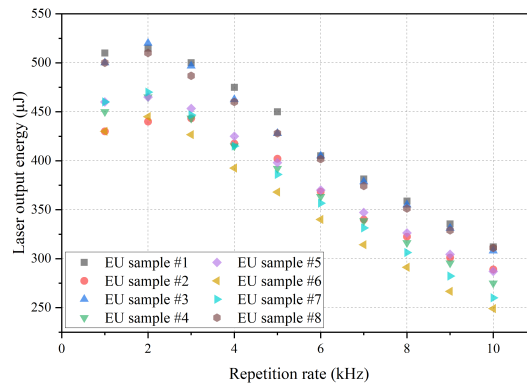


Figure 3: Laser output energy as a function of the pulse repetition rate at a fixed absorbed pump power.

Keeping the same optimization procedure (adjustment of pump focus position and delay time), the cavity-dumped laser output energy was measured as a function of the repetition rate, which was varied between 1 kHz and 10 kHz. The absorbed pump power was set to 27 W. Again, the pulse duration was 2.8 ns for all repetition rates. As it can be seen in Figure 3, laser operation with pulse energies over 250 μJ could be achieved over the whole PRF range. Furthermore, a nearly constant offset of maximum 80 μJ consists between the measurements of the different crystals for all PRF and corresponds to the existing offset of the laser output energy at 27 W (compare Figure 2a). The overall behavior of the laser output energy as a function of the PRF is similar for all crystals. A maximum appears at a PRF of 2 kHz (except for the measurement with EU sample #2 with the maximum at around 3 kHz) with a mean decreasing slope of  $-25 \pm 2 \mu\text{J}/\text{kHz}$  afterwards.

#### 4. COMPARISON STUDY OF EU AND NON-EU CRYSTALS

To classify the European GALACTIC crystals within the global market, a comparison study with crystals from two non-European suppliers was carried out. For this, the laser performance study at 5 kHz was repeated with the US samples #1 and 2# as well as with the Chinese samples #1 and #2. The absorbed pump power was again only increased to 27 W to avoid damage, and the crystal temperature was set to 30°C. The laser output energies measured with the non-European crystals are depicted in Figure 4a. To enable a direct comparison, the highest and the lowest achieved result of the EU samples are also shown (EU samples #1 and #2). The highly doped non-EU crystals (US sample #2 and Chinese sample #2) showed an output energy characteristic very similar to the GALACTIC crystals. Small deviations could be again caused by adjustments. A different behavior was observed with the low-doped crystals. Here, the laser output energy curves of both low-doped crystals have a significantly smaller slope efficiency compared to the highly doped crystals. By looking at the results achieved with the crystals from the US supplier for example, the resulting output energy obtained with sample #1 is 25 % lower than with sample #2 at an absorbed pump power of 27 W. This behavior can be explained by the pump

optic design, which was chosen to guarantee the best mode matching for the highly doped crystals in a doping range of 0.2-0.22 at%. This is achieved, if the confocal parameter of the focused pump beam matches with the absorption length of the crystal, which amounts to 2 mm for a doping concentration of 0.2 at%. Since crystals with a doping concentration of 0.13 at% have a longer absorption length of around 3.5 mm, the overlap between pumped volume and laser mode is worse and, thus, the output energy was also expected to be lower. Therefore, the direct comparison of the GALACTIC and the non-European crystals is of course only reasonable if similar doping concentrations are used.

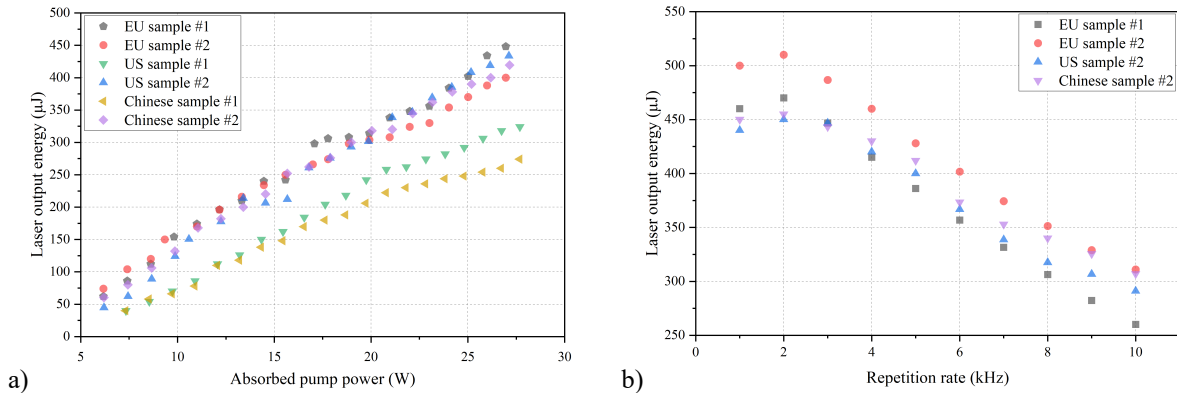


Figure 4: Comparison of the laser results measured with the EU and the non-EU crystals; a) Laser output energy as a function of the absorbed pump power; b) Variation of the pulse repetition rate.

The variation of the PRF between 1 kHz and 10 kHz was chosen as a second measurement for the comparison study. The resulting curves for all highly doped crystals are depicted in Figure 4b. In total, all tested samples show the same behavior for increasing PRF. Nevertheless, differences can be seen in the decreasing slope after the maximum output energy at 2 kHz for all crystals. The comparative study presented here demonstrated a similar quality of the crystals and optical coatings in comparison to the crystals manufactured from the non-EU suppliers. At this point, it can be concluded that the crystals with a doping concentration of 0.2 at% manufactured in the course of the GALACTIC project have reached competitiveness on the global market.

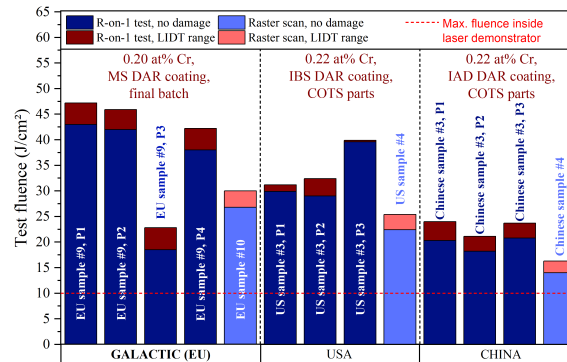


Figure 5: LIDT test results of the coated crystals from the GALACTIC consortium and the two non-EU suppliers.

LIDT measurements were performed with an OPO pumped by a diode-pumped Nd:YAG laser and appropriate beam steering, polarization and focusing optics. The resulting test beam had a wavelength of 750 nm, a pulse duration of ~3.5 ns and a  $1/e^2$  beam diameter of ~230 μm. Since the standard S-on-1 LIDT test according to ISO 21524 was not possible in this case because of the available sample size and amount of samples (the S-on-1 test would require a total test surface comparable with that of a Ø 25 mm optic), the test procedure comprised on the one hand an R-on-1 test on three positions and on the other hand a raster scan on a 3 x 3 mm<sup>2</sup> test area. Two highly doped samples from each supplier as well as from the GALACTIC crystals were used, since the small square geometry was not large enough to perform both tests on one sample. The R-on-1 test was used to determine the range of the damage threshold for the subsequent raster scan via irradiation of three positions with 1000 laser shots at a constant fluence. Then the fluence was stepwise increased until a

damage occurred. For the raster test, the sample was scanned with overlapping laser pulses (14 pulses per beam diameter) at a constant fluence. Afterwards, the fluence was again raised step-by-step, and the raster movement was repeated for each fluence level as long as no damage was observed. This method was very sensitive to small LIDT critical defects with low surface density (few defects per sample), because it tested the whole central part of the optical surface.

The results from all tested crystals are illustrated in the bar graph in Figure 5. In order to compare the resistivity against intense laser irradiation of the samples from the different manufacturers, the highest fluence level before a damage occurred (blue bars) and the LIDT range (red area) are determined for each R-on-1 test and raster scan. The GALACTIC crystals (EU sample #9 & EU sample #10) show the highest LIDT with over 40 J/cm<sup>2</sup> for the R-on-1. Since locally limited defects can strongly affect the measured LIDT value, which explains the low LIDT measured at position P3 in comparison to the results achieved at P1 and P2, the R-on-1 test was repeated at a fourth position P4. The GALACTIC crystals also show the highest values for the raster scan with over 25 J/cm<sup>2</sup>. The lowest damage thresholds were determined with the Chinese samples. Here, it has to be noted, that different coating methods were used for the non-EU samples (see Figure 5), which could also influence the achievable LIDT values. Since only dense, sputtered coatings – i.e. manufactured via the MS or IBS coating technology – are proven to be suitable for space applications, the GALACTIC crystals are potentially suited for the use in space missions, which is additionally confirmed by the LIDT values achieved here.

## 5. SUMMARY

In this work, we presented on the one hand the laser results achieved with the Alexandrite crystals manufactured within the GALACTIC project to verify the reproducibility of the crystal and coating quality and on the other hand a comparison study with samples from two non-European suppliers.

To verify the reproducibility, eight GALACTIC samples were tested in a cavity-dumped Q-switched laser system and the resulting laser performance was compared. Similar curves with a maximum deviation of  $\pm 7\%$  could be detected for the measured output energy as a function of the absorbed pump power. Larger differences were found regarding the laser wavelength, which could be attributed to small variations in the alignment of the crystal and cavity as well as variations due to the coating deposition. Nevertheless, the different spectral characteristics did not affect the laser output energy. Moreover, the variation of the repetition rate from 1 to 10 kHz only showed a maximum deviation of 8% at 10 kHz. The tests have proven the reproducibility of the Alexandrite crystals manufactured in the GALACTIC project and have shown the good quality of the final development state. High output energies could be achieved without observing any type of damage, which shows their robustness and suitability for high power applications.

Furthermore, the comparison study with crystals from two non-European suppliers (USA and China) could demonstrate the competitiveness of the GALACTIC crystals on the global market, which could be reinforced by achieving the highest LIDT values.

Funding: European Union's Horizon 2020 research and innovation programme under grant agreement no 870427

## REFERENCES

- [1] J. C. Walling, O. G. Peterson, H. P. Jenssen, R. C. Morris, and E. W. O'Dell, "Tunable Alexandrite Lasers," *IEEE J. Quant. Electron.* 16(12), 1302–1315 (1980).
- [2] J. W. Kuper, T. Chin, and H. E. Aschoff, "Extended tuning range of Alexandrite at elevated temperatures," *Proc. Advanced Solid State Lasers (OSA)* 6, paper CL3 (1990).
- [3] A. Munk, B. Jungbluth, M. Strotkamp, H.-D. Hoffmann, R. Poprawe, J. Höffner, and F.J. Lübken, "Diode-pumped alexandrite ring laser in single-longitudinal mode operation for atmospheric lidar measurements," *Proc. of SPIE Vol. 11180, 1118029-1 – 1118029-8* (2018).
- [4] A. Munk, M. Strotkamp, B. Jungbluth, J. Froh, T. Mense, A. Mauer, and J. Höffner, "Rugged diode-pumped Alexandrite laser as an emitter in a compact mobile lidar system for atmospheric measurements," *J. Appl. Optics* 60 (16), 4668-4680 (2021).
- [5] J. Lauterbach, J. Höffner, P. Menzel, and P. Keller, "The new scanning iron LIDAR, current state and future developments," *Proc. of the 17th ESA Symposium on European Rocket and Balloon Programmes and Related Research, Sandefjord, Norway*, 327 – 329 (2005).

- [6] G. M. Thomas, A. Minassian, X. Sheng, M. J. Damzen, “Diode-pumped Alexandrite lasers in Q-switched and cavity-dumped Q-switched operation,” *Optics Express*, vol. 24 (24), 27212 (2016).
- [7] ILT press release, “Collecting complex climate data thanks to compact alexandrite lasers,” 05 December 2019, <https://www.ilt.fraunhofer.de/en/press/press-releases/press-release-2019/press-release-2019-12-5.html>
- [8] Cordis Europa, Horizon2020, Fact Sheet: “High Performance Alexandrite Crystals and Coatings for High Power Space Applications,” <https://cordis.europa.eu/project/id/870427>
- [9] Project website, <https://h2020-galactic.eu/>
- [10] P. Weßels, S. Unland, R. Kalms, S. Spiekermann, H. Mädebach, S. Kramprich, L. Jensen, D. Kracht, M. Lorrai, P.G. Lorrai, M. Hmidat, J. Butkus, L. Lukosevicius, and J. Neumann, “GALACTIC – High Performance Alexandrite Crystals and Coatings for High Power Space Applications,” *Proc. SPIE Vol. 11852 118526S* (2021).
- [11] G. Tawy, and M. J. Damzen, “Tunable, dual wavelength and self-Q-switched Alexandrite laser using crystal birefringence control,” *Optics Express* 27 (13), 17507 (2019).